PAPER • OPEN ACCESS

Surface Wave Tomography Using Seismic Ambient Noise Data for Subsurface Imaging beneath Bandung Basin, West Java and Its Surrounding

View the article online for updates and enhancements.

IOP ebooks™

Bringing you innovative digital publishing with leading voices to create your essential collection of books in STEM research.

Start exploring the collection - download the first chapter of every title for free.

Surface Wave Tomography Using Seismic Ambient Noise Data for Subsurface Imaging beneath Bandung Basin, West Java and Its Surrounding

Sri Dwi Wuryani [1]*, Tedi Yudistira [2], Sri Widiyantoro[2]

[1]Master Program of Geophysical Engineering, Institut Teknologi Bandung, Jalan Ganesha No. 10, Bandung 40132, Indonesia
[2]Department of Geophysical Engineering, Institut Teknologi Bandung, Jalan Ganesha No. 10, Bandung 40132, Indonesia

*corresponding author's email : wuryani.dwis@gmail.com

Abstract. Seismic interferometry was applied to estimate the shear wave velocity structure beneath the Bandung Basin, West Java. The empirical Green's function (EGFs) were obtained by cross-correlate each pairs of seismic stations from the temporary seismic network installed in the research area. In this research, we use Rayleigh wave dispersion data as the input for surface wave tomography. The obtained dispersion curves of Rayleigh waves are in the period range 1 - 12 s. The dispersion characteristics of EGFs was also analyzed to estimate the distribution of the ambient noise sources. Based on the symmetricity characteristics of the dispersive signals of EGFs from all two station pairs oriented relatively in N-S and W-E the seismic noise sources was originated from oceanic activity at the Coastline of Java Sea. Furthermore, the dispersion curves also show that the group velocities vary within range of 1.6 – 2 km/s. The inverted dispersion data into depth models provide the variation of shear velocity structures at depth 1 – 5 km in the range of 1 – 2.1 km/s. At depth 1 – 4 km, there appear high and low velocity contrast in the south of Mt. Tangkuban Perahu, which is may be related to the existence of Lembang Fault. Meanwhile, velocity models at depth 1 – 3 km show the lateral variation of shear wave's velocity in the Bandung Basin. The high velocity structures within range 1.8 – 2.1 km/s lies in the Southwest toward Northeast in the middle of Bandung Basin. This structures divide Bandung Basin into two parts, Western part and Eastern part.

1. Introduction

Interferometry is a subsurface imaging method, conducted by cross-correlating signal recorded by two seismic stations to obtain a new signal, known as Green's Function. Surface waves interferometry for subsurface imaging had been well-known since the basic theory first introduced by [1]. In the last few decades, researches by using this method has developed in order to extract the Green's Function, not only from microseismic ambient noise signal but also from coda wave and direct wave signals [2]. Over the past few years, ambient noise interferometry had been performed to identify subsurface structure in Indonesia [3–6], in local and regional scale area.

In this research, we conducted ambient noise interferometry in local scale to identify subsurface velocity structures beneath Bandung Basin, West Java and its surrounding. The method used to obtain Rayleigh waves group velocity dispersion curves was based on research by [7]. By analysing the shear wave's velocity in Bandung Basin and its surrounding, we might be able to contribute in the investigation of the hazard potential, such as landslide, especially in the North of Bandung Basin and

near Lembang Fault, which maybe happened in the future. We are interested to determine the shear wave's velocity structures by approximated them with Rayleigh wave group velocity analysis. The subsurface velocity structure was estimated by applying inversion method which has developed by [8].
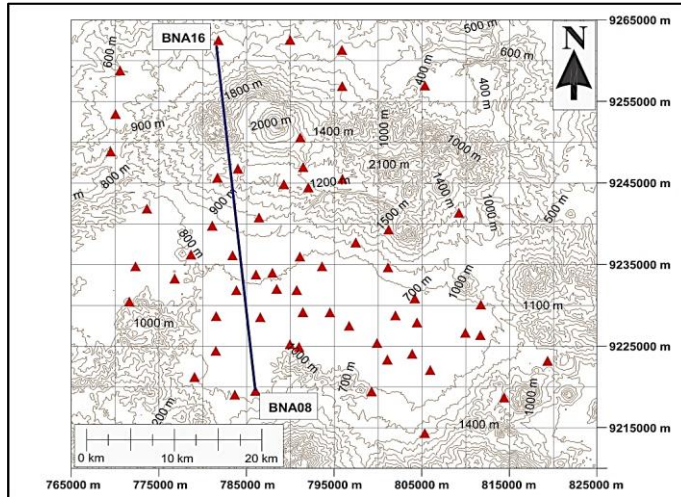

Figure 1. Temporary seismic network with sparse coverage in the Northern area (around Mt. Tangkuban Perahu) and denser coverage in Bandung Basin.

We used the waveform data from the seismic network contains of 59 seismic stations, which are temporary installed in around Bandung Basin and Mt. Tangkuban Perahu (Figure 1). The data contains daily recorded waveform within about 8 months recording period. We only analysed the vertical component data to recover the Green's Function from Rayleigh waves. Green's Function can be obtained by taking time derivative of the cross-correlation function. The positive lag part ($\hat{G}_{AB}(t)$ ($t \geq 0$)) is known as causal, while the negative lag part ($\hat{G}_{BA}(-t)$ ($t \leq 0$)) is known as anti-causal.

$$-\hat{G}_{AB}(t) + \hat{G}_{BA}(-t) = \frac{dC_{AB}(t)}{dt} \tag{1}$$

Empirical Green's Function (EGF) can be obtained by cross correlating noises which are the accumulation of diffusive plane waves from recorded signal between two receivers. The asymmetry in Green's Functions are not caused by the large earthquake distribution, but they're related to the origin and the distribution of the ambient noises sources. The EGFs contain the dispersive signals which can be approximated by far-field wave propagation for Rayleigh waves to obtain the dispersion curves of phase or group velocity.

2. Methods

We followed the procedure for ambient noise data processing introduced by [9]. First, we did the single data preparation. This step includes mean removal, trend removal, temporal normalization and spectral whitening. We normalized the signal by applying a 'one-bit' normalization and a bandpass filter within range $0.02 - 1$ Hz to reduce the effect of earthquake signals to the waveform and those only left the ambient noise signals. The second step is cross-correlated and stacked the multiple connecting band to obtain a new broadband signal, called Green's Function. The measurement of Rayleigh waves velocity dispersion curves were performed by frequency-time analysis (FTAN) methods. From the 59 seismic stations, we obtained 1522 EGFs but only 1218 dispersion curves were extracted. Dispersion curves were extracted by using image transformation technique [10] and Multiple Filter Technique (MFT) [11].

All the procedures from single data preparation to dispersion curves extraction were done through a MATLAB programs that were implemented by [10]. To the 3-D shear waves velocity models were inverted by using the DSurfTomo program [8], which is a direct inversion program based on the fast marching ray tracing method [12] and wavelet-based sparsity-constrained inversion technique [13]. This program allows to conduct an inversion processes to obtain a shear waves velocity model as the function of depth, directly from dispersion curves without reconstructing shear waves tomographic

velocity maps. Checkerboard test was also conducted to evaluate the lateral resolution of shear wave's velocity model. We used grid model constructed by 30x30 grid nodes with interval 0,017° horizontally and 21 vertical nodes with several interval (0.5 km for depth 0 – 5 km, 1 km for depth 6 – 10 km and 2.5 km for depth 10 – 15 km). We added 2% of random noise to synthetic data and inverted them to determine whether the checkerboards were fully or poorly recovered. The initial model itself was a laterally homogenous with shear velocity is 1 km/s at depth 0 km and the velocity increased by 0.075 km/s as the depth increased by 1 km. After performing some trial-and-error test, we obtained the best resolution at the smoothing and damping factor by 1.5 with reliable results of shear velocity models at depth 1 – 5 km.

3. Results and Discussions

We analyzed Empirical Green's Functions in different period ranges (1-5 s, 5-10 s, 10-15 s, 15-20 s and >20 s). Then we compare the EGFs from station pairs relatively oriented in North-South (N-S) (Figure 2) and West-East (W-E) (Figure 3) with ±15° deviation. The cross-correlation resulted EGFs with clear dispersion signals in period 1 - 12 s, which are within microseismic band. In the period 1 - 5 s, the dispersive signals are present in causal part for station pairs in relatively N-S, but symmetric for station pairs in relatively W-E. Similar pattern also presents in the period 5 - 10 s, where the dispersive signals clearly appear in the causal part of EGFs for N-S pairs and symmetric for the W-E pairs.
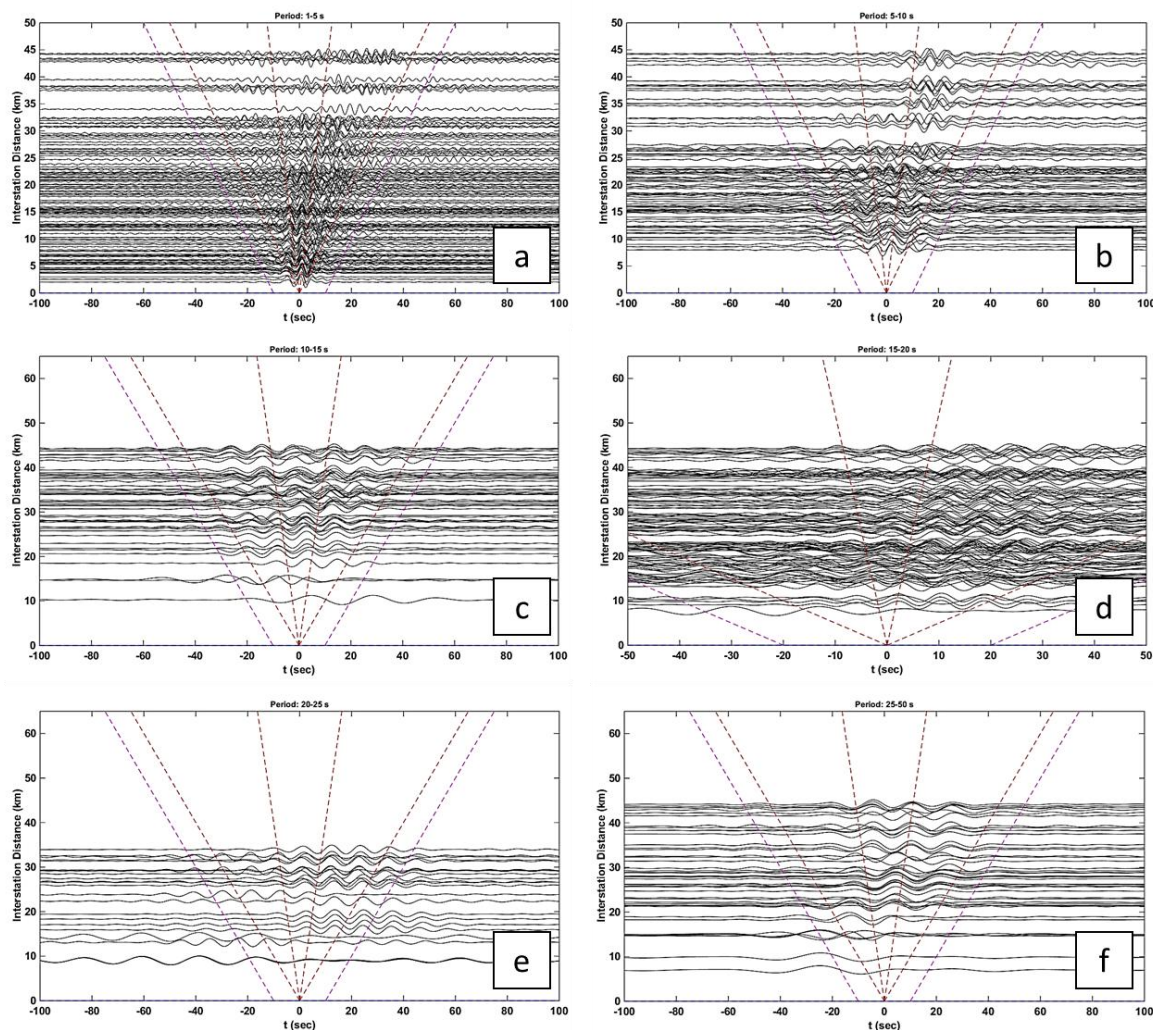

Figure 2. EGFs for stations pairs oriented relatively in N-S with deviation ±15° at period (a) 1-5 s, (b) 5-10 s, (c) 10-15 s, (d) 15-20 s, (e) 20-25 s, and (f) 25-50 s.

In period 10 - 15 s, the dispersive signals in both N-S and W-E pairs are seems symmetric at causal and anti-causal part of EGFs and the amplitudes are not too clear. In the period 15-20 s, the dispersive signals with low amplitudes are slightly present in the causal part of N-S pairs and in the anti-causal part of W-E pairs. In the period 20-25 s, EGFs in the N-S and W-E pairs show the low amplitude dispersive signals in causal part. For higher period (>20 s), the dispersive signals are not clear in both N-S and W-E pairs. Based on this results, we determined that ambient noises recorded by temporarily installed seismic network in the investigation area are in microseismic band and the origin was predicted as oceanic activities in Java Sea. As for the higher period, we couldn't exactly predict the origin of the signals since the dispersive signals are not clearly identified.

We chose only EGFs with SNR>5 and interstation distances are two times of wavelength ($\Delta > 2\lambda$) to extract dispersion curves and those we obtained 1218 curves. The dispersion curves show average Rayleigh waves group velocity within range 1.6 – 2 km/s for period 1 – 12 s (Figure 4). The shear wave's velocity models were obtained after we directly inverted the dispersion data into shear wave's velocity models. The results of the inversion process are shown in figure 5.
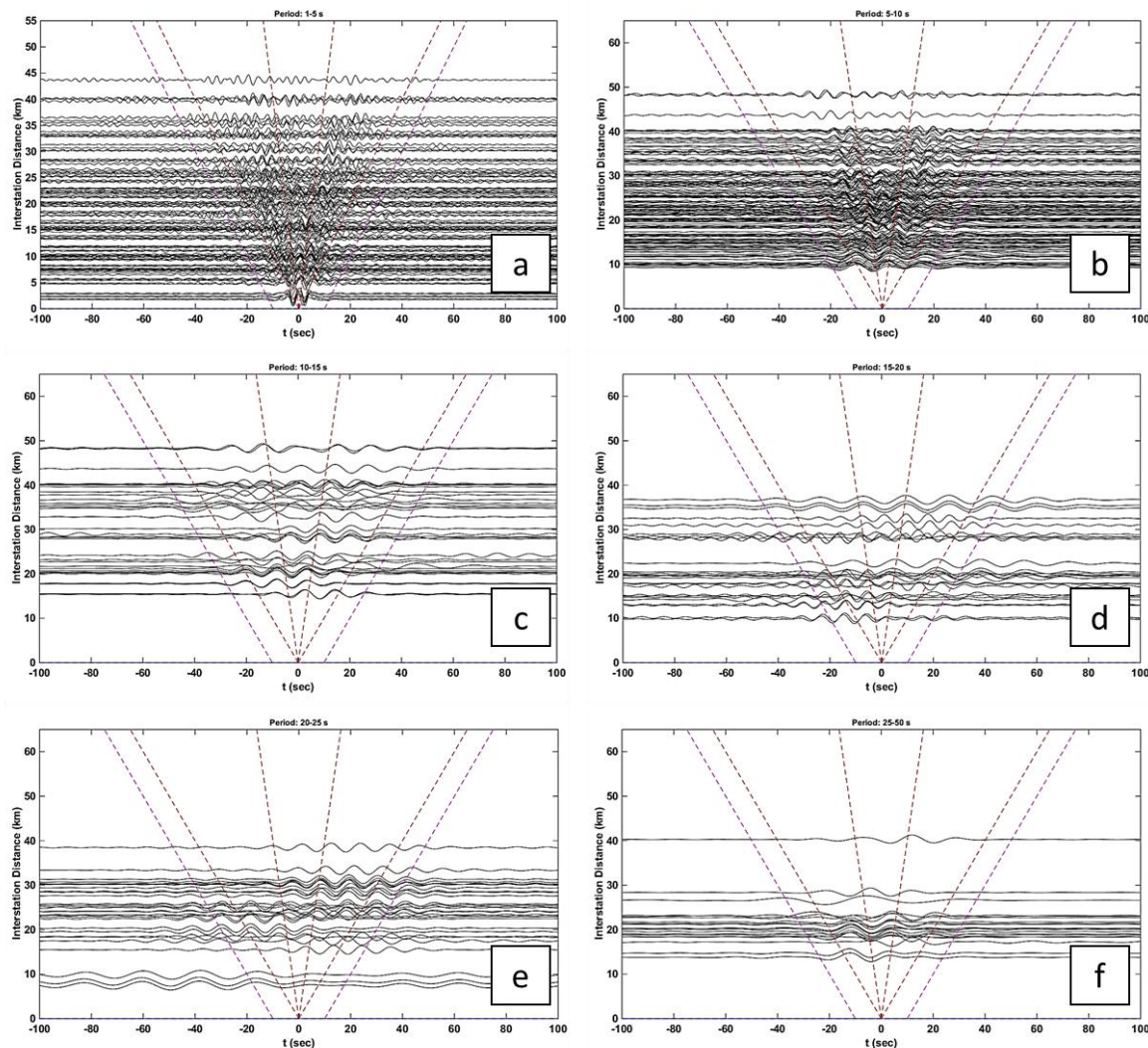

Figure 3. EGFs for stations pairs oriented relatively in W-E with deviation ±15° at period (a) 1-5 s, (b) 5-10 s, (c) 10-15 s, (d) 15-20 s, (e) 20-25 s, and (f) 25-50 s.
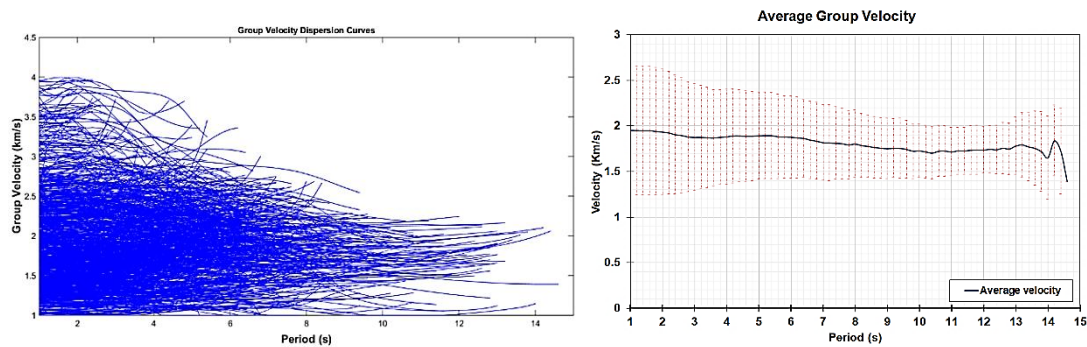
Figure 4. Rayleigh waves group velocity dispersion curves and the average of group velocity in around the investigation area covered by this research.

The inverted shear wave's velocity models at figure 5 show the lateral variation of shear wave's velocity within range of 0.9 – 2.1 km/s at depth of 1 – 5 km. The models show a clear the lateral variation of shear wave's velocity structures in around the investigation area at depth 1 – 4 km but the intensity was lower at 5 km depth. The velocity models roughly show that the shear velocity values increase with depth. A high velocity structures within range of 1.8 – 2.1 km/s was identified in the middle of Bandung Basin at depth 1 – 3 km. It is oriented in Southwest-Northeast and lies from Dayeuhkolot toward Ujung Berung. This structure divides Bandung Basin which has shear wave velocity about 0.9 – 1.5 km/s into two parts, western part and eastern part.
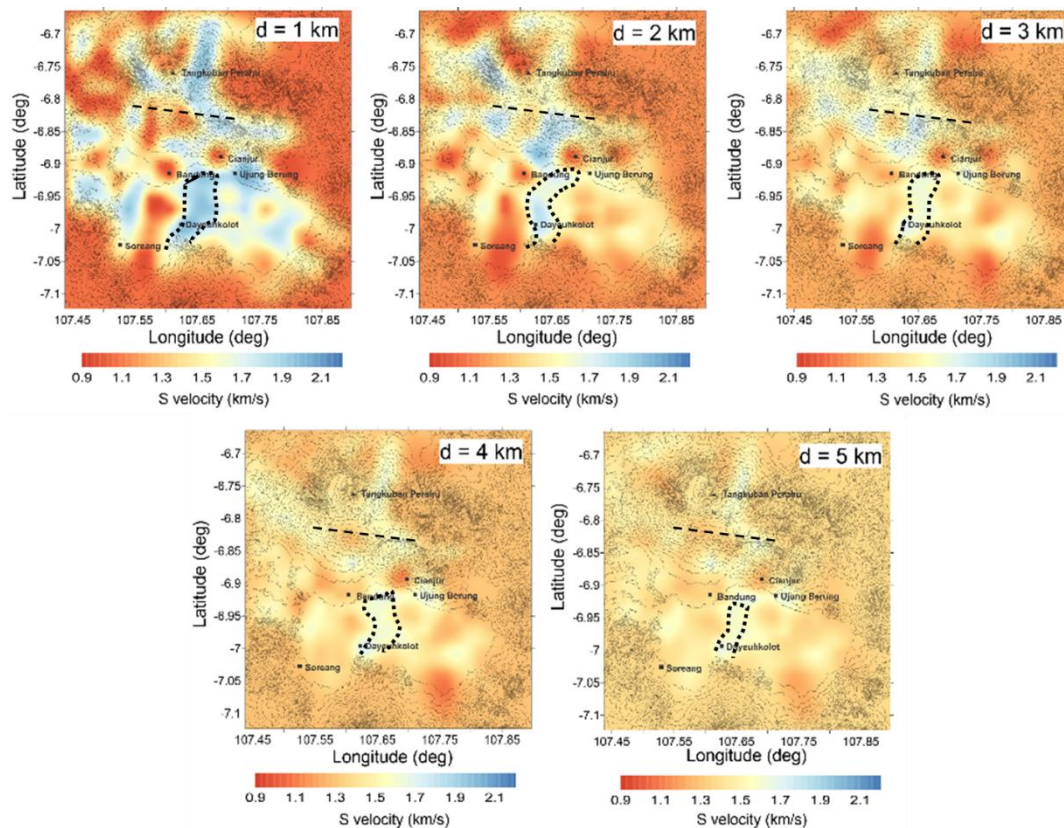

Figure 5. Shear wave's velocity model at depth 1 – 5 km.

In the north of Bandung Basin, the anomaly contrast of high and low shear velocity was identified in around Lembang Fault. This contrast lies in depth 1 – 4 km with higher shear velocity in the southern area. We predicted that this anomaly contrast was related to the existence of the normal fault oriented in west-east, called Lembang Fault. Furthermore, around Mt. Tangkuban Perahu, a low velocity structures are present at depth 1 – 2 km and we predicted that this anomaly is related to the volcanic activities beneath Mt. Tangkuban Perahu.

4. Conclusions

We have determined the EGFs from the cross-correlation of ambient seismic noise recorded by temporarily installed seismic network in the Bandung Basin, West Java, Indonesia. We obtained that the dispersive signals at period 1-12 s, which the origin is predicted as the oceanic activity in Java Sea. As the origin of signals with the higher period are unable to predict since the dispersive signals aren't clearly appeared at EGFs. The calculated group velocity was vary at 1.6 – 2 km/s. The dispersion curves show a wide range of group velocity at period 1 – 3 and gradually narrower at longer period with consistency in curve's trend.

The inverted models from Rayleigh waves group velocity dispersion curves show the variation of shear wave velocity at depth 1 -5 km. Generally, the shear wave's velocity increases with depth. At depth 1 – 4 km, an anomaly contrast presents in between Mt. Tangkuban Perahu dan Bandung Basin with high velocity structures are more in the southern area than the low velocity structure. This structures are may be related to the existence of Lembang Fault. Meanwhile at depth 1 - 3 km, there is a high velocity structure with velocity range at 1.8 – 2.1 km/s and oriented in southwest to northeast, lies from Dayeuhkolot toward Ujung Berung. This anomaly divides Bandung Basin which has shear velocity structure about 0.9 – 1.5 km/s into two parts, the western part and eastern part.

5. References

[1]   Claerbout J F 1968 Synthesis of a layered medium transmission from its acoustic transmission response *Geophysics* **33** 264–9

[2]   Yao H, Campman X, de Hoop M V. dan van der Hilst R D 2009 Estimation of surface wave Green's functions from correlation of direct waves, coda waves, and ambient noise in SE Tibet *Phys. Earth Planet. Inter.* **177** 1–11

[3]   Putriastuti M, Yudistira T, Dian Nugraha A, Widiantoro S dan Metaxian J-P 2017 Ambient Noise Tomography of Merapi Complex, Central Java, Indonesia: A Preliminary Result *IOP Conf. Ser. Earth Environ. Sci.* **62**

[4]   Martha A A, Cummins P, Saygin E, Sri Widiyantoro dan Masturyono 2017 Imaging of upper crustal structure beneath East Java–Bali, Indonesia with ambient noise tomography *Geosci. Lett.* **4**

[5]   Zulfakriza Z, Saygin E, Cummins P R, Widiyantoro S, Nugraha A D, Lühr B G dan Bodin T 2014 Upper crustal structure of central Java, Indonesia, from transdimensional seismic ambient noise tomography *Geophys. J. Int.* **197** 630–5

[6]   Saygin E, Cummins P R, Cipta A, Hawkins R, Pandhu R, Murjaya J, Masturyono, Irsyam M, Widiyantoro S dan Kennett B L N 2016 Imaging architecture of the Jakarta Basin, Indonesia with transdimensional inversion of seismic noise *Geophys. J. Int.* **204** 918–31

[7]   Yao H, Van Der Hilst R D dan de Hoop M V 2006 Surface-wave array tomography in SE Tibet from ambient seismic noise and two-station analysis - I. Phase velocity maps *Geophys. Journal-Oxford* **166** 732–44

[8]   Fang H, Yao H, Zhang H, Huang Y C dan Van Der Hilst R D 2015 Direct inversion of surface wave dispersion for three-dimensional shallow crustal structure based on ray tracing: Methodology and application *Geophys. J. Int.* **201** 1251–63

[9]   Bensen G D, Ritzwoller M H, Barmin M P, Levshin A L, Lin F, Moschetti M P, Shapiro N M dan Yang Y 2007 Processing seismic ambient noise data to obtain reliable broad-band surface wave dispersion measurements *Geophys. J. Int.* **169** 1239–60

[10]   Yao H, Xu G, Zhu L dan Xiao X 2005 Mantle structure from inter-station Rayleigh wave dispersion and its tectonic implication in western China and neighboring regions *Phys. Earth Planet. Inter.* **148** 39–54

[11]   Dziewonski A, Bloch S dan Landisman M 1969 A technique for the analysis of transient seismic signals *Bull. Seismol. Soc. Am.* **59** 427–44

[12]   Rawlinson N dan Sambridge M S 2005 The fast marching method: an effective tool for tomographic imaging and tracking multiple phases in complex layered media *Explor. Geophys.* **36** 341–50

[13]   Fang H dan Zhang H 2014 Wavelet-based double-difference seismic tomography with sparsity regularization *Geophys. J. Int.* **199** 944–55